ORIGINAL CONTRIBUTION

# Efficiency of Washout Ratio during Dynamic MR Imaging in Acute Osteoporotic and Metastatic Compression Fractures of Vertebral Bodies

Hiroaki TAKEUCHI, Junta HARADA, Shinpei TADA

*Department of Radiology, Jikei University, School of Medicine*
*3-25-8, Nishi-Shimbashi, Minato-ku, Tokyo 105-8461*

The purpose of our study was to evaluate the efficiency of washout ratio during dynamic MRI in the diagnosis of acute osteoporotic and metastatic compression fractures of vertebral bodies. Thirty-three acute osteoporotic and metastatic compression fractures in 40 patients were studied using $T_1$-weighted images, $T_2$*-weighted images and Gd-DTPA dynamic enhanced study with spin echo sequences. Time-intensity curves were obtained and the washout ratio was calculated. After the dynamic studies, gadolinium enhanced $T_1$-weighted images were obtained. Washout ratios calculated in cases of osteoporotic fractures ranged from 0.0000 to 0.3634 (mean $0.122 \pm 0.114$, 1 standard deviation). In cases of metastatic fracture, the washout ratio ranged from 0.1573 to 0.7393 (mean $0.426 \pm 0.169$, 1 standard deviation). There was a significant difference in the calculated washout ratios for cases of osteoporotic fracture and cases of metastatic fracture (Student's t-test, $p < 0.0001$). In conclusion, these findings suggest that washout ratio may be of value in the differentiation between acute osteoporotic and metastatic fractures.

## INTRODUCTION

Differentiation of acute osteoporotic from metastatic compression fractures of vertebral bodies is a common problem and sometimes difficult. To differentiate them is important for treatment planning in patients with known malignancy. Magnetic resonance (MR) imaging can provide useful information in diagnosis[1),2)]. But about signal intensity of compressed vertebral bodies, acute osteoporotic compression fractures and metastatic fractures show low signal intensity on $T_1$-weighted images and high intensity on $T_2$-weighted images[1),3),4)]. In contrast chronic osteoporotic compression fractures of vertebral bodies show normal signal intensity[5)]. Gadolinium-enhanced MR imaging has been found to increase diagnostic reliability, although increased signal intensity is seen in both acute osteoporotic and

**Keywords** dynamic MR imaging, washout ratio, osteoporosis, metastasis, compression fractures of vertebral bodies

metastatic vertebral bodies after gadolinium injection[6]. However, unenhanced and gadolinium-enhanced MR imagings do not always allow a definite differentiation of acute osteoporotic from metastatic compression fractures. In these situations, we thought, from our clinical experience, that washout ratio during dynamic MR imaging can provide valuable additional information. Since, to our knowledge, similar studies have not been reported previously.

## MATERIALS AND METHODS

We retrospectively studied 73 compression fractures of vertebral bodies with lower signal intensity than that of adjacent normal vertebrae on $T_1$WI in 40 patients (19 men, 21 women ; mean age ± one standard deviation, 65.6 years ± 11.8 ; range, 32～83 years). All patients underwent MR imaging within less than 3 weeks after the onset of pain, and had pain at the time of MR imaging. Thirty-three cases of osteoporotic compression fractures of vertebral bodies in 21 patients and 40 cases of metastatic compression fractures in 19 patients were studied in our institution. The primary sites of carcinoma were bronchi (n=6), liver (n=3), breast (n=2), kidney (n=2), colon (n=1), stomach (n=1), uterus (n=1), testicle (n=1), small bowel (n=1), and prostate (n=1).

Verification of osteoporotic fractures was achieved by clinical history and observations of more than 18 months of follow up periods because pathological proof was not obtained. Metastatic fractures in 4 patients were proven by biopsy (1 case), operative findings (2 cases), or autopsy (1 case). Verification of metastatic fractures in the other 15 patients with known primary carcinoma were achieved by progressive deterioration of a fractured vertebra or involvement of other vertebrae on follow-up radiographic examinations (as evidenced by bone destruction, bone marrow replacement, or a soft tissue mass).

MR imaging was performed with a 0.2–T system (MRP–20 ; Hitachi Medical Co., Tokyo) equipped with a solenoid coil. $T_1$–weighted spin echo sequences were performed at 500/25/5 (repetition time (TR)/echo time (TE)/excitations) and a section thickness of 7.5 mm with a 0.5 mm gap. $T_2$*–weighted gradient-echo sequences were obtained with a 500/25, 30° flip angle and a section thickness of 10 mm with no gap. These sequences were performed with a 256 × 192 imaging matrix. Both studies were followed by dynamic imaging obtained with spin echo sequences, which were obtained at 200/25/2, a section thickness of 10 mm and a 256 × 160 imaging matrix. One image was acquired every 58–64 seconds. Section orientations were selected to represent the largest low-signal-intensity area in compressed vertebral bodies on sagittal images. After the initial image, a bolus of Gd-DTPA (0.1 mmol/kg body weight) was manually injected intravenously via a 20–gauge plastic cannula. Nine serial images were acquired. After the dynamic studies, gadolinium-enhanced $T_1$–weighted spin echo sequences were performed at 500/25, with a section thickness of 7.5 mm, a 0.5 mm gap, and a 256 × 192 imaging matrix. All sequences were obtained with a field of view of 280 mm.

Received Spt. 1, 1997 ; revised Nov. 12, 1997
Reprint requests to Hiroaki Takeuchi, Department of Radiology, Jikei University, School of Medicine, 3–25–8, Nishi-Shimbashi, Minato-ku, Tokyo 105–8461

Region of interest (ROI) analysis was applied to the dynamic spin echo images. ROIs were plotted with elliptically shaped in collapsed vertebral bodies where $T_1$ weighted images showed low signal intensity with increased intensity after injection of Gd-DTPA. Collapsed vertebral bodies showed very inhomogeneous enhancement patterns when reviewed dynamically. Measurements were therefore obtained from multiple ROIs within lesions. For each lesion, the maximally enhanced region was used to calculate washout ratio. To obtain the time-intensity curves, measurements were performed from each ROI. Time-intensity curves were generated by normalizing ROI signal intensity to base line values as the 'enhancement index' (mean ROI pixel signal intensity from post contrast image/ mean ROI pixel signal intensity from pre contrast image). Washout ratio was calculated as follows : 1–enhancement index at 9 minutes/ maximal enhancement index during dynamic images. ROIs were also plotted in 33 non-compressed vertebral bodies where $T_1$– and $T_2$*–weighted images showed isosignal intensity in 21 patients. To obtain the time-intensity curves of apparently normal vertebral bodies, measurements were performed from each ROI.

## RESULTS

1) Gadolinium-enhanced and -unenhanced MR imaging.

Homogeneous or inhomogeneous low signal intensity, as compared with the signal intensity of adjacent normal vertebrae, was found in both kinds of compression fractures of vertebral bodies on $T_1$–weighted imagies, high signal intensity in both kinds of compression fractures on $T_2$*–weighted imagings (Table 1). Isointensity was seen only in osteoporotic compression fractures of vertebral bodies (21 cases, 64%) after injection of Gd-DTPA (Table 1). Predictive values were shown in Table 2.

Horizontal low signal intense zones on $T_1$–weighted images, horizontal high signal intense zones on $T_2$*–weighted images, horizontal increased signal intense zones on Gd-enhanced $T_1$–weighted images and retropulsed bone fragments were seen only in osteoporotic compres-

Table 1. Signal Intensity Characteristics in MR Imagings of Osteoporotic and Metastatic Compression Fractures of Vertebral Bodies

| | Signal intensity* | metastatic fractures (n=40) | osteoporotic fractures (n=33) |
|---|---|---|---|
| $T_1$-weighted Images | Low intense homogeneous | 30 (75) | 19 (58) |
| | inhomogeneous | 10 (25) | 14 (42) |
| $T_2$–weighted Images | High intense homogeneous | 31 (78) | 12 (36) |
| | inhomogeneous | 9 (22) | 21 (64) |
| Gadolinium-enhanced | Low intense homogeneous | 11 (27) | 6 (18) |
| $T_1$-weighted Images | inhomogeneous | 29 (73) | 6 (18) |
| | Iso intense homogeneous | | 7 (21) |
| | inhomogeneous | | 14 (43) |

Note-Numbers are numbers of fractures.
Percentages are in parenthesis.
* Compared with the signal intensity of adjacent normal vertebra in the same patient.

sion fractures. On the other hand, pedicle involvement and paravertebral masses appeared only in metastatic compression fractures (Table 2). Convex shaped posterior walls of compressed vertebral bodies were suggesting metastatic fractures (Table 2). The predictive values of gadolinium-enhanced and unenhanced MR findings were shown in Table 3.

2) Dynamic MR Imagings and washout ratio.

Osteoporotic compression fractures were characterized by an early peak with slightly decreased intensity on delayed images (Fig. 1). On the other hand, metastatic compression fractures generally had an early peak with large decreased intensity (Fig. 2). The mean time intensity curve during dynamic MR imaging was shown in Fig. 3. Normal vertebral bodies

Table 2. MR Imaging Findings Predictive of Osteoporotic and Metastatic Compression Fractures of Vertebral Bodies

| | metastatic fractures (n=40) | osteoporotic fractures (n=33) | Sensitivity (%) | Specificity (%) | PPV (%) | NPV (%) |
|---|---|---|---|---|---|---|
| Osteoporotic | | | | | | |
| Horizontal low signal intense zone on $T_1$ WI | | 10 | 30 | 100 | 100 | 37 |
| Horizontal high signal intense zone on $T_2$ WI | | 8 | 24 | 100 | 100 | 38 |
| Horizontal increased signal intense zone on Gd-enhanced $T_1$ WI | | 8 | 24 | 100 | 100 | 38 |
| Iso intense on Gd-enhanced $T_1$ WI | | 21 | 64 | 100 | 100 | 23 |
| Retropulsed bone fragment | | 2 | 6 | 100 | 100 | 44 |
| Metastatic | | | | | | |
| Convex shaped posterior wall of compressed vertebral body | 7 | 2 | 18 | 95 | 78 | 59 |
| Pedicle involvement | 11 | | 28 | 100 | 100 | 53 |
| Paravertebral mass | 14 | | 35 | 100 | 100 | 63 |

Note-Numbers are numbers of fractures.
WI=weighted images.
Gd-enhanced $T_1$ WI=Gadolinium-enhanced $T_1$ weighted images.
PPV=positive predictive value.
NPV=negative predictive value.

Table 3. Gadolinium-enhanced and unenhanced MR findings Predictive of Osteoporotic and Metastatic Compression Fractures of Vertebral Bodies

| Static MR findings | metastatic fractures (n=40) | osteoporotic fractures (n=33) | Sensitivity (%) | Specificity (%) | PPV (%) | NPV (%) |
|---|---|---|---|---|---|---|
| Osteoporotic | | 23 | 70 | 100 | 100 | 80 |
| Metastatic | 18 | 4 | 45 | 88 | 82 | 57 |

Note-Numbers are numbers of fractures.
PPV=positive predictive value. NPV=negative predictive value

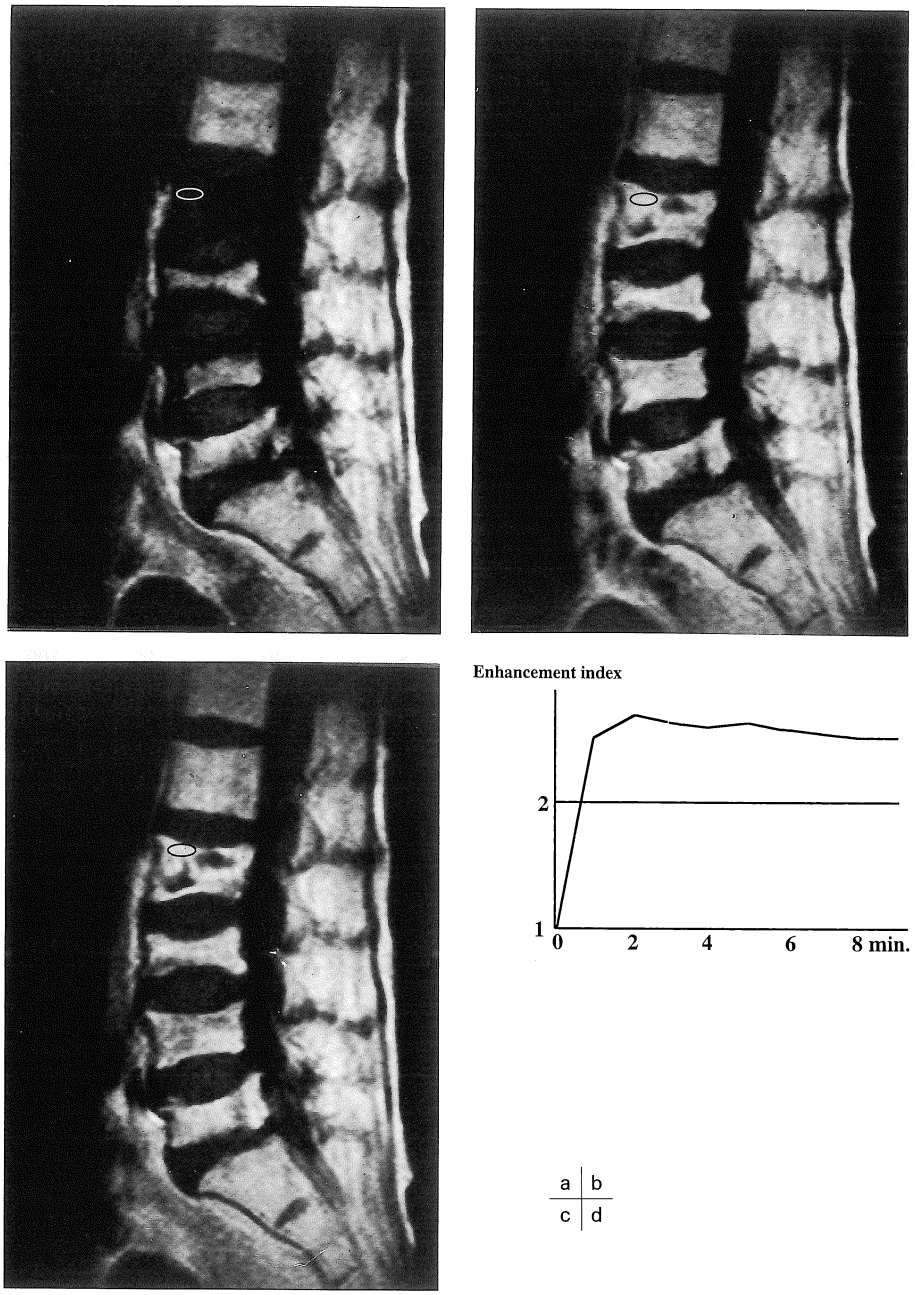


Fig. 1. Dynamic MR images of osteoporotic compression fractures of vertebral bodies. A elliptically region of interest was plotted in compressed vertebral body.
(a) The initial sagittal image showed a markedly decreased signal intensity in the compressed second,third and fifth lumbar vertebra.
(b) An image at two minutes after the injection of Gd-DTPA showed markedly inhomogeneous enhancement in compressed vertebral bodies.
(c) An image at nine minutes after the injection of Gd-DTPA showed a slight decrease in intensity in compressed vertebral bodies, compared with an image at two minutes.
(d) Diagram of the time intensity curve showed an early peak with little decrease in intensity on delayed images.

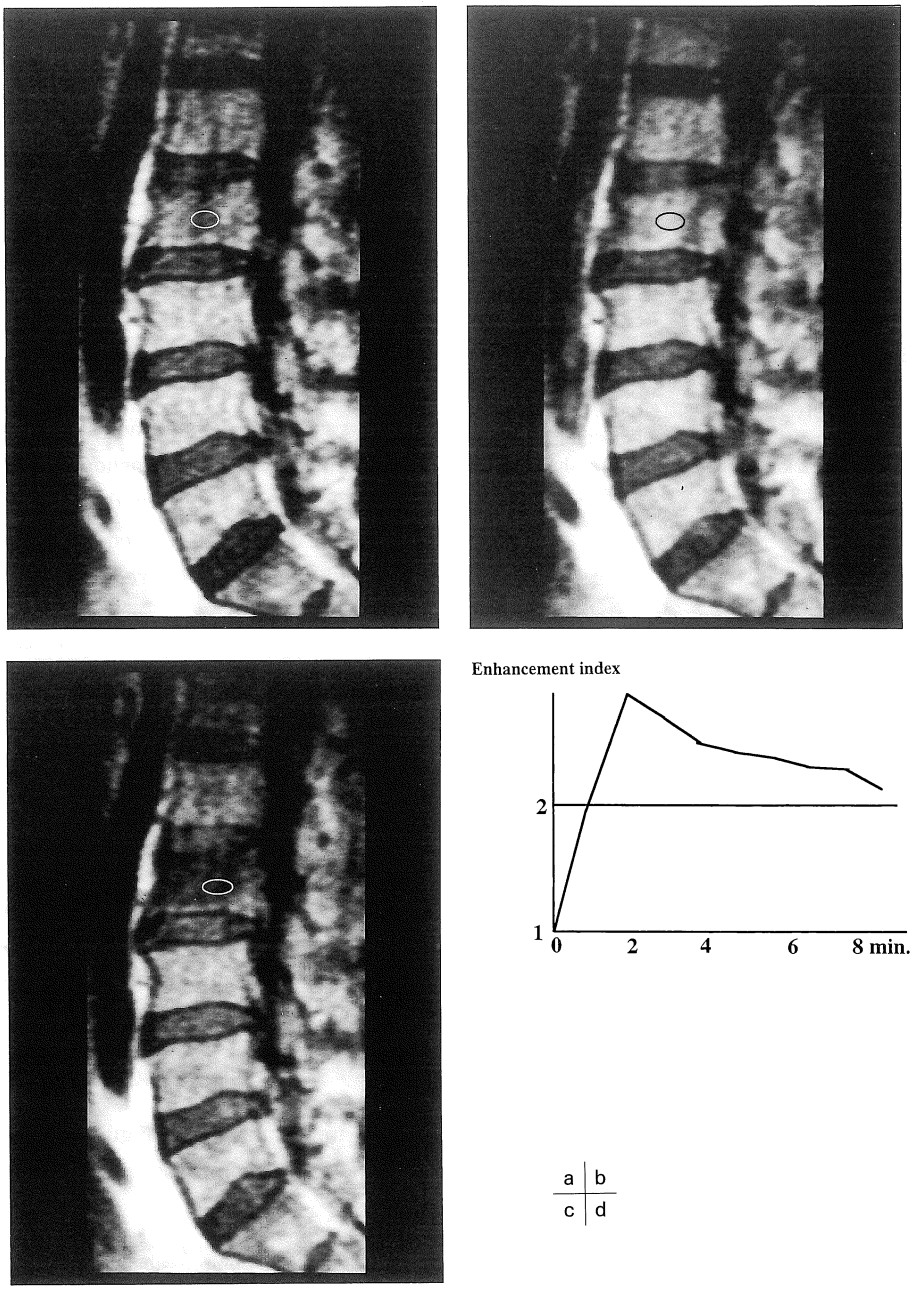


Fig. 2. Dynamic MR images of metastatic compression fractures of vertebral bodies. The primary tumor was colon carcinoma. A elliptically region of interest was plotted in compressed vertebral body.
(a) The initial sagittal image showed a markedly decreased signal intensity in the compressed second lumbar vertebral body.
(b) An image at two minutes after the injection of Gd-DTPA showed marked enhancement in compressed vertebral body.
(c) An image at nine minutes after the injection of Gd-DTPA showed decreased signal intensity in compressed vertebral body compared with an image at two minutes.
(d) Diagram of time intensity curve showed an early peak with large decrease in intensity on delayed images.

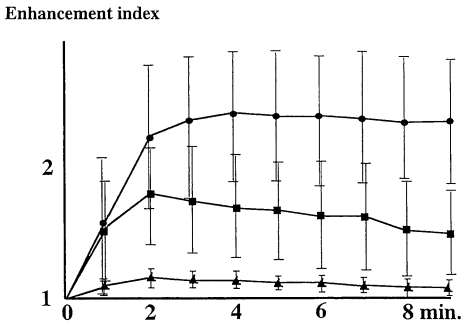


Fig. 3. Diagram of mean enhancement index measurements in osteoporotic compression fractures of vertebral bodies (circles, n=33), metastatic (squares, n=40) and normal vertebral bodies (triangles, n=33) were shown. Error bars (±1 standard deviation) were described in each measurements.

showed only minimal enhancement (Fig. 3).

Washout ratio of osteoporotic fractures as follows, mean : 0.122, one standard deviation : 0.114, range : 0.0000～1.3634. Washout ratios of metastatic fractures were as follows, mean : 0.426, one standard deviation : 0.169, range : 0.1573～0.7393. There was a significant difference between the washout ratios of metastatic and osteoporotic fractures (Student's t-test, $p<0.0001$). Most washout ratios of osteoporotic fractures were smaller than 0.25, and most washout ratios of metastatic fractures were larger than 0.25 (Table 4). When osteoporotic fractures were defined as having a washout ratio of less than 0.25, the sensitivity and specificity were both 88%. The positive predictive value was 85% and the negative predictive value was 90%. When metastatic fractures were defined as having a washout ratio of more than 0.25, the sensitivity and specificity were both 88%. The positive predictive value was 88% and the negative predictive value was 85% (Table 5).

Table 4. Washout Ratio of Osteoporotic and Metastatic Compression Fractures of Vertebral Bodies

| | metastatic fractures (n=40) | osteoporotic fractures (n=33) |
|---|---|---|
| Washout Ratio≦0.25 | 5 | 29 |
| Washout Ratio>0.25 | 35 | 4 |

Note-Numbers are numbers of fractures.

Washout ratios of 8 cases of metastatic fractures whose primary tumors were H.C.C. and R.C.C. were as follows, mean : 0.450, one standard deviation : 0.42, range : 0.1573～0.7393. Washout ratios of the other 32 cases of metastatic fractures were as follows, mean : 0.420, one standard deviation : 0.26, range : 0.1684～0.6782. The difference between the washout ratios of these two groups was not significant (Mann-Whitney's U-test, $p>0.8$).

## DISCUSSION

It is important to distinguish osteoporotic from metastatic compression fractures as soon

Table 5. Washout Ratio Predictive of Osteoporotic and Metastatic Compression Fractures of Vertebral Bodies

| | Sensitivity (%) | Specificity (%) | PPV (%) | NPV (%) |
|---|---|---|---|---|
| Osteoporotic (Washout Ratio≦0.25) | 88 | 88 | 85 | 90 |
| Metastatic (Washout Ratio>0.25) | 88 | 88 | 88 | 85 |

Note-PPV=positive predictive value. NPV=negative predictive value

as possible, because to select the appropriate treatment promptly is good effect for the quality of life of patients, especially those with metastatic compression fractures. MR imaging is useful in evaluating numerous pathologic conditions of the spine[7)~9)], and is recommended as the initial technique of choice in patients suspected to have metastatic spinal disease[10),11)], because it is the most sensitive procedure available for identifying bone marrow metastases to the spine[12)]. Several authors have shown that metastatic involvement of the spine is best imaged by a combination of $T_1$– and $T_2$–weighted images[13),14)]. Modic et al.[14)] stated that neoplasms involving the vertebral column characteristically had low signal intensity on $T_1$– weighted images and high signal intensity on $T_2$–weighted images. Recently however, several authors have shown that signal intensity, on $T_1$– or $T_2$–weighted images is not diagnostic of metastatic lesions of the spine[12),15)]. Moreover, others have shown that benign compression fractures may have low signal intensity on $T_1$–weighted images similar to malignant lesions[3),15),16)]. However, Cuenod et al.[6)] reported that signal intensity analysis and morphologic analysis of unenhanced and gadolinium-enhanced MR imagings are useful to distinguish them. Our results showed some kind of signal intensity analysis and morphologic analyses are valuable to predict cause of compression fractures (Table 1). Unfortunately their appearance rates were low, therefore low sensitivity and low negative predictive value were obtained (Table 2, 3).

Most washout ratios of metastatic fractures were larger than the washout ratios of osteoporotic fractures (Fig. 1, 2, Table 4). We presumed that the reasons were derived from the proportion of vascularity, cellularity and interstitial components.

In studies of the response of osteosarcomas to preoperative chemotherapy, static enhanced $T_1$–weighted images overestimated the amount of residual viable tumor[17),18)], because images of non-neoplastic fibroblastic tissue or non-malignant granulation tissue may enhance after Gd-DTPA infusion[16),17)]. Fukuda et al.[19)] found that enhancement after contrast injection on spin-echo images do not always indicate a poor response to chemotherapy, most enhanced areas consist of postnecrotic granulation tissue and loose fibrotic tissue with proliferation of dilated small vessels. They also found that the early phase of dynamic MR imaging after a bolus injection of contrast medium could be used to delineate tumor vascularity in the largest tumor cut plane. Tumor vascularity and staining on angiography were found to reflect viable tumor cells[20),21)].

As for vertebral bodies of compression fractures, we presume that enhancement due to postnecrotic granulation tissue and loose fibrotic tissue with proliferation of dilated small vessels continues in both osteoporotic and metastatic compression fractures similar to osteosarcomas after chemotherapy[17)~19)]. The presense of necrotic tissue was proved by operative specimen in our study. Tan et al. found that biopsy specimens taken from vertebral bodies with benign compression fractures contained marrow fibrosis and acute osteonecrosis[15)]. We also assume that the early peak seen on MR images was caused by infiltration of bone marrow by metastatic tumors (Fig. 3), similar to osteosarcoma[17)~19)]. Metastatic compression fractures consequently tended to have a lower washout ratio whereas osteoporotic compression fractures had a higher washout ratio.

Our study was performed with a 0.2–T system. A 1.5–T system may be better suited for dynamic MR studies[22]. Furthermore a more suitable dynamic time intensity curve may be obtained by using a fast gradient echo sequence with a 1.5T–system.

We had assumed that characteristics such as vascularity of the primary tumor site would significantly influence the washout ratio. However, we found no significant difference in washout ratio between metastatic compression fractures whose primary tumors were H.C.C. and R.C.C. which generally are hyper vascular tumors, and those whose primary tumors were of other kinds. Differences in vascularity of the primary tumors apparently had no significant influence on washout ratio.

Acute osteoporotic compression fractures show decreased signal intensity on $T_1$–weighted images[5], whereas chronic osteoporotic compression fractures show normal signal intensity on $T_1$–weighted images[3),4)]. The signal strength of osteoporotic compression fractures changes with time, consequently the washout ratio of osteoporotic compression fracture may also change with time. But our study was performed immediately after patients of osteoporotic compression fractures felt pain. Our study was initiated early after the onset of osteoporotic compression fractures. We thought that there was apparently no significant changes in washout ratio with time in our study.

When osteoporotic fractures were defined as having a washout ratio less than 0.25, and metastatic fractures were defined as having a washout ratio greater than 0.25, good predictability of osteoporotic and metastatic compression fractures were obtained (Table 5).

Gadolinium-enhanced and -unenhanced MR imagings do not always allow a confident differentiation of osteoporotic from metastatic compression fractures (Table 3). We therefore believe that the washout ratio during dynamic MR imaging may provide valuable additional information.

## REFERENCES


1) Baker LL, Goodman SB, Perkash I, et al. : Benign versus pathologic compression fractures of vertebral bodies : assessment with conventional spin-echo, chemical-shift, and STIR MR imaging. Radiology 1990 ; 174 : 495–502
2) Yuh WTC, Zachar CK, Barloon TJ, et al. : Vertebral compression fracture : distinct between benign and malignant causes with MR imaging. Radiology 1989 ; 172 : 215–218
3) Sugimura K, Yamasaki K, Kitagaki H, Tanaka Y, Kono M : Bone marrow diseases of the spine : differentiation with $T_1$ and $T_2$ relaxation times in MR imaging. Radiology 1987 : 165 : 541–544
4) Frager D, Elin C, Swerdlow M, et al. : Subacute osteoporotic compression fracture : misleading magnetic resonance appearance. Skeletal Radiology 1988 ; 17 : 123–126
5) Colman LK, Porter BA, Redmond JI, et al. : Early diagnosis of spinal metastases by CT and MR studies. J Comput Assist Tomogr 1988 ; 12 : 423–426
6) Cue'nod CA, Laredo JD, Chevret S, et al. : Acute vertebral collapse due to osteoporosis or malignancy : appearance on unenhanced and gadolinium-enhanced MR images. Radiology 1996 ; 199 : 541–549
7) Beltran J, Simon DC, Levy M, et al. : Aneurysmal bone cysts : MR imaging at 1.5 T. Radiology 1986 ; 158 : 689–690
8) Williams AL, Haughton VM, Pojunas KW, et al. : Differentiation of intramedullary neoplasms and cysts by MR. AJR 1987 ; 149 : 159–164
9) Zimmer WD, Berquist TH, Mcleid RA, et al. : Bone tumors : Magnetic resonance imaging versus computed tomography. Radiology 1985 ; 155 : 709–718

10) Godersky JC, Smoker PK, Knutzon R : Use of magnetic resonance imaging in the evaluation of metastatic spinal disease. Neurosurgery 1987 ; 21 : 676–680
11) Norman D : The spine. In : Brant-Zawadzki M, Norman D, ed. Magnetic Resonance Imaging of the Central Nervous System. First ed. New York, USA : Raven Press, 1987 ; 289–328
12) Avrahami E, Tadmor R, Dally O, et al. : Early MR demonstration of spinal metastases in patients with normal radiographs and CT and radionuclide bone scan. J Comput Assist Tomogr 1989 ; 13 : 598–602
13) Chafetz N, Genant HK, Gillespy T, et al. : Magnetic resonance imaging. In : Kricun ME, ed. Imaging Modalities in Spinal Disorders. First ed. Philadelphia, USA : WB Saunders, 1988 ; 478–502
14) Modic MT, Masark TJ, Paushter D : Magnet resonance imaging of the spine. Radiol Clin North Am 1986 ; 24 : 229–245
15) Tan SB, MBBS, MMed, et al. : The limitations of magnetic resonance imaging in the diagnosis of pathologic vertebral fractures. Spine 1991 ; 16(8) : 919–923
16) Frager D, Elkin C, Swerdlow M, et al. : Subacute osteoporotic compression fractures : misleading magnetic resonance appearance. Skeletal Radiol 1988 ; 17 : 123–126
17) Hanna SL, Parham DM, Fairclough DL, et al. : Assessment of osteosarcoma response to preoperative chemotherapy using dynamic FLASH gadolinium DTPA-enhanced magnetic resonance mapping. Invest Radiol 1992 ; 27 : 367–373
18) Erlemann R, Sciuk J, Bosse A, et al. : Response of osteosarcoma and Ewing sarcoma to preoperative chemotherapy : assessment with dynamic and static MR imaging and skeletal scintigraphy. Radiology 1990 ; 175 : 791–796
19) Fukuda K, Irie T, Hata Y, et al. : MRI Evaluation of preoperative chemotherapy in osteosarcomas : signal intensity changes and contrast enhancement effects. Jpn J Magn Reson 1991 ; 11 : 364–372
20) Chuang VP, Benjamin R, Jaffe N, et al. : Radiographic and angiographic changes in osteosarcoma after intraarterial chemotherapy. AJR 1982 ; 139 : 1065–1069
21) Carrasco CH, Charnsangavej C, Raymond AK, et al. : Osteosarcoma : angiographic assessment of response to preoperative chemotherapy. Radiology 1989 ; 170 : 839–842
22) Hittmair K, Turetschek K, Gomiscek G, Stiglbauser R, Schmirawitzki H : Field strengh dependence of MRI contrast enhancement : phantom measurements and application to dynamic breast imaging. Br J Radiology 1996 ; 69 : 215–220